JACS
JOURNAL OF THE AMERICAN CHEMICAL SOCIETY
Article
pubs.acs.org/JACS

Orbital-Resolved Partial Charge Transfer from the Methoxy Groups of Substituted Pyrenes in Complexes with Tetracyanoquinodimethane—A NEXAFS Study

Katerina Medjanik,[†,*] Dennis Chercka,[‡] Peter Nagel,[§] Michael Merz,[§] Stefan Schuppler,[§] Martin Baumgarten,[‡] Klaus Müllen,[‡] Sergej A. Nepijko,[†] Hans-Joachim Elmers,[†] Gerd Schönhense,[†] Harald O. Jeschke,[∥] and Roser Valenti[∥]

[†]Institut für Physik, Johannes Gutenberg-Universität Mainz, 55099 Mainz, Germany
[‡]Max-Planck-Institut für Polymerforschung, Postfach 3148, 55021 Mainz, Germany
[§]Karlsruhe Institute of Technology (KIT), Institut für Festkörperphysik, 76021 Karlsruhe, Germany
[∥]Institut für Theoretische Physik, Goethe-Universität Frankfurt, 60438 Frankfurt am Main, Germany

Supporting Information

ABSTRACT: It is demonstrated that the near-edge X-ray absorption fine structure (NEXAFS) provides a powerful local probe of functional groups in novel charge transfer (CT) compounds and their electronic properties. Microcrystals of tetra-/hexamethoxypyrene as donors with the strong acceptor tetracyano-*p*-quinodimethane (TMP/HMP-TCNQ) were grown by vapor diffusion. The oxygen and nitrogen K-edge spectra are spectroscopic fingerprints of the functional groups in the donor and acceptor moieties, respectively. The orbital selectivity of the NEXAFS pre-edge resonances allows us to precisely elucidate the participation of specific orbitals in the charge transfer process. Upon complex formation, the intensities of several resonances change substantially and a new resonance occurs in the oxygen K-edge spectrum. This gives evidence of a corresponding change of hybridization of specific orbitals in the functional groups of the donor (those derived from the frontier orbitals 2*e* and 6a_1 of the isolated methoxy group) and acceptor (orbitals b_{3g}, a_u, b_{1g}, and b_{2u}, all located at the cyano group) with π*-orbitals of the ring systems. Along with this intensity effect, the resonance positions associated with the oxygen K-edge (donor) and nitrogen K-edge (acceptor) shift to higher and lower photon energies in the complex, respectively. A calculation based on density functional theory qualitatively explains the experimental results. NEXAFS measurements shine light on the action of the functional groups and elucidate charge transfer on a submolecular level.

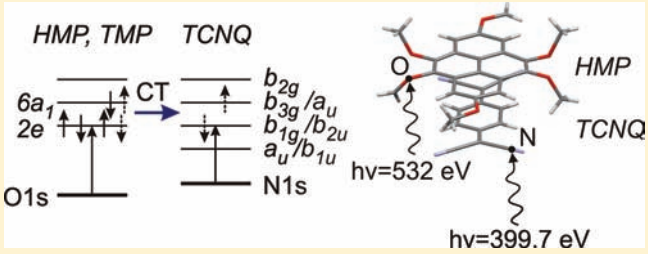

INTRODUCTION

Functionalized Polycyclic Aromatic Hydrocarbons with Strong Acceptor or Donor Character. In the field of molecular electronics, conjugated organic molecules have received intense attention as n-type or p-type semiconductors. In particular, charge transfer (CT) compounds of molecules with tailored donor and acceptor character provide a vast multitude of design possibilities. Understanding the electronic structure of this class of materials is crucial for designing specific electrical properties. In particular, large planar polycyclic aromatic hydrocarbon molecules with different functional groups at the periphery have recently been studied intensively. It was shown that their electronic properties can be tailored for strong electron acceptor or donor character.[1] Novel chemical synthesis routes, as described for coronene, by Rieger et al.[2] paved the way toward the design of a new class of donor and acceptor molecules both based on the same parent molecule. Indeed, donor hexamethoxycoronene and acceptor coronene–hexaone codeposited in ultrahigh vacuum (UHV) form a weak CT complex, as recently shown using photoemission.[3]

Likewise, the pyrene molecule can be functionalized at its periphery by adding either methoxy or keto groups, thus yielding moderate donors or strong acceptors, respectively. The donor moieties are of particular interest because their sizes are similar to that of the classical acceptor *7,7,8,8-tetracyano-p-quinodimethane* (TCNQ, $C_{12}N_4H_4$). In *4,5,9,10-tetramethoxypyrene* (TMP, $C_{20}H_{18}O_4$) the four functional groups lower the ionization potential (IP) to 5.47 eV, indicating an increased donor character in comparison with the parent molecule pyrene (IP 7.41 eV).[4] In *2,4,5,7,9,10-hexamethoxypyrene* (HMP, $C_{22}H_{22}O_6$), IP is further lowered to 5.17 eV, as measured by cyclovoltammetry. The newly prepared donors TMP and HMP were purified by column chromatography (silica/toluene) and fully characterized before trying to cocrystallize them (details to

Received: October 26, 2011
Published: February 9, 2012

   dx.doi.org/10.1021/ja2100802 | *J. Am. Chem. Soc.* 2012, 134, 4694–4699

be published elsewhere). It is thus interesting to investigate the possible formation of new CT complexes based on these donor moieties, in particular in compounds with TCNQ. Thin films of the TMP-TCNQ complex on atomically clean gold surfaces produced by UHV codeposition have been investigated by ultraviolet photoelectron spectroscopy (UPS) and scanning tunnelling spectroscopy (STS), revealing shifts of the valence levels upon complex formation.[5] However, a participation of specific orbitals in the charge transfer could not be deduced from these measurements in the valence region.

Charge Transfer Salts Studied via Near-Edge X-ray Absorption Fine Structure (NEXAFS) Spectroscopy. NEXAFS is a powerful tool for the investigation of organic molecules, which can be good candidates for the formation of new CT complexes.[6−11] In NEXAFS (see Stöhr in ref 12 for details on the method) measurements an electron is excited from a core level to an empty or partially unoccupied valence state. As this technique gives direct access to the unoccupied density of states (DOS), it should be sensitive to the formation of new hole states due to charge transfer in a donor−acceptor complex.[13] For the TMP/HMP-TCNQ complexes the nitrogen and oxygen K-edge spectra are ideal, because these atomic species are located exclusively on the acceptor site (nitrogen in the cyano groups of TCNQ) or the donor site (oxygen in the methoxy groups of TMP and HMP). In the present study we exploited soft X-rays from the WERA beamline at ANKA, Karlsruhe, at an energy resolution of 190 meV. In the total electron yield mode employed, the drain current from the sample is detected. The electron emission yield originates from a subsequent Auger process that neutralizes the core hole and leads to the emission of Auger electrons and slow secondary electrons. The information depth is about 5 nm. The interlayer spacing is of the order of 0.33 nm; see data in the Supporting Information. The probing depth thus corresponds to approximately 15 molecular layers, which is sufficient for yielding information on the bulk of the crystallites.

Fraxedas et al.[14] performed a NEXAFS study of the classical CT salt tetrathiafulvalene (TTF, $C_6S_4H_4$)−TCNQ. This compound forms parallel segregated stacks of donors (TTF) and acceptors (TCNQ). Results have been compared with a first-principle calculation of the unoccupied and partially occupied electronic states of the pure materials and the CT compound. Sing et al.[15] studied the same system with a focus on the renormalized band widths observed in UPS.[16,17] The symmetry of the observed orbitals for TCNQ was probed, and information on molecular orientation was gained.[15] None of these papers addressed the issue of a possible change of the unoccupied density of states upon formation of the CT complex.

In the present paper we present NEXAFS results for solution-grown 3D microcrystals of the complexes TMP-TCNQ and HMP-TCNQ. Crystallites with sizes in the 100 μm range were grown by vapor diffusion of hexane into a dichloromethane solution of a 1:1 mixture of the components, and the compound crystals (looking dark) were separated from crystals of the pure moieties (transparent for the donors and light green for TCNQ) with a micromanipulator. The structure was analyzed by X-ray analysis (for structure plots, see the Supporting Information). TMP-TCNQ cocrystals are stacking in an alternate fashion. The symmetric distance (0.332 nm) of TCNQ to a TMP on top and a TMP below reveals that no dimerization occurs. Neighboring alternating stacks show a TMP donor next to a donor and a TCNQ acceptor next to an acceptor, such that layers of donors and layers of acceptors are formed. Since the HMP-TCNQ crystallites used for NEXAFS were too small for X-ray analysis, we performed an X-ray analysis for larger cocrystals with one intercalated dimethyl sulfoxide (DMSO, C_2H_6OS) molecule per donor−acceptor pair (HMP-TCNQ·DMSO). In this case some methoxy groups are heavily twisted out of the plane by 65−85° (see Supporting Information).

RESULTS AND DISCUSSION

Nitrogen and Oxygen K-Edge NEXAFS Spectra. NEXAFS spectra have been taken for the dark fractions of the microcrystals, deposited on carbon tape. Typical results for the nitrogen and oxygen K-edge spectra are shown in Figure 1.

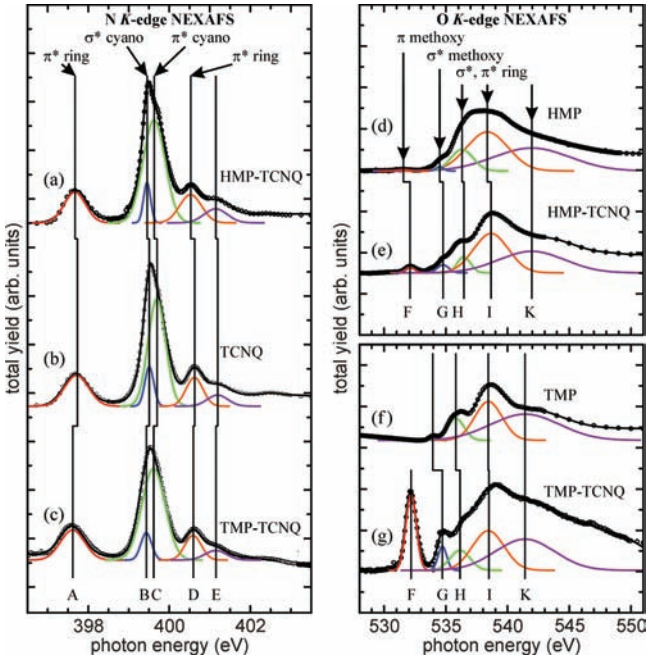

Figure 1. Left panel: Nitrogen K-edge NEXAFS spectra of the HMP/TMP-TCNQ complexes (a, c) and of pure TCNQ (b). Circles denote experimental data; thin curves below the spectra mark partial spectra of the transitions as obtained from a multipeak fit routine; curves through the dots represent the sum of the partial spectra. Right panel: Same for the K-edge spectra of oxygen. Spectra (d, f) were taken for pure HMP and TMP, respectively; spectra of complexes (e, g) correspond to the same samples as (a, c) in the left panel. The yield scales are normalized to the areas of peaks A (left panel) and I (right panel).

The spectral features (A−E for nitrogen and F−K for oxygen) were quantitatively analyzed by a multipeak fit routine, assuming a mixed Gaussian/Lorentzian function (80%/20%) accounting for a finite energy resolution of 0.19 eV and a lifetime broadening of 0.4 eV. The partial spectra are shown as thin lines, circles denote the measurement and lines through the circles denote the sum spectra. As nitrogen is present only in the cyano groups of TCNQ, its edge fine structure is a fingerprint of the acceptor. Likewise, oxygen is only contained in the methoxy groups, and thus, its spectrum reflects a local spectroscopic probe in the functional group of the donor.

Nitrogen K-Edge NEXAFS. The spectra for the nitrogen K-edge (Figure 1, left panel) were deconvoluted into signals A−E by the fit routine. In all spectra the fit curve perfectly

dx.doi.org/10.1021/ja2100802 | J. Am. Chem. Soc. 2012, 134, 4694−4699

reproduces the data points, giving evidence of a high reliability of the partial spectra. We briefly recall the peak assignment for NEXAFS spectra of pure TCNQ from ref 14. The first signal A is a π^*-type resonance (full width at half-maximum (fwhm 630 meV)) associated with the lower a_u and b_{1u} orbitals. These originate from the degenerate pair of lowest empty π^*-orbitals of the benzene core, which only slightly delocalize toward the cyano group in TCNQ. We denote the transition of this signal as A: N 1s → a_u, b_{1u} (π^* *ring*). At photon energies in resonance with such an allowed dipole transition, a large increase in excitation cross section is observed (see transition scheme in Figure 2). Signals B and C originate from p-type unoccupied

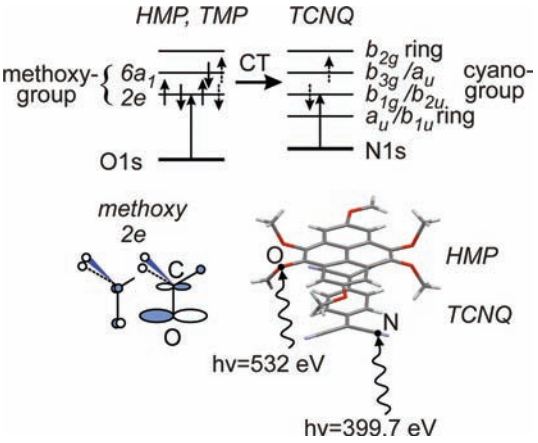

Figure 2. Scheme of the NEXAFS transitions involving the frontier orbitals of the methoxy groups in HMP or TMP (symmetry 2e and 6a_1 for an isolated methoxy group) as charge-donating orbitals and b_{1g}/b_{2u} and b_{3g}/a_u of the cyano group of TCNQ as accepting orbitals. Bottom left, structure of the 2e-orbital of an isolated methoxy group.[18]

orbitals located in the cyano group. They are therefore higher in intensity due to the larger overlap with the N 1s wave function in the dipole matrix element. B is a narrow resonance (fwhm 210 meV) of σ^*-type originating from the b_{1g} and b_{2u} orbitals that belong to the four symmetry adapted combinations of in-plane orbitals of the cyano groups CN, denoted B: N 1s → b_{1g}, b_{2u} (σ^* *cyano*). Signal C is of π^*-type and is much broader (645 meV). It derives from the b_{3g} and a_u orbitals and is denoted as C: N 1s → b_{3g}, a_u (π^* *cyano*). Signal D corresponds to the highest π^*-type orbital of benzene (b_{2g}) that is delocalized over the whole TCNQ molecule, D: N 1s → b_{2g} (π^* *ring*). The weak feature E originates from delocalized σ^*-type orbitals containing σ^*(C−C), σ^*(C−H), and σ^*(C≡N) contributions. In summary, the final states involved in the weaker transitions A and D are delocalized on the benzene ring, whereas states involved in transitions B, C, and part of E derive from the σ^*- and π^*-orbitals of the cyano group. We have checked the σ^* and π^* character of signals B and C by angle-resolved measurements on thin films.

In the spectra of the two complexes a and c in Figure 1, the intensities of signals B and C are significantly smaller than those for pure TCNQ. This intensity drop upon complex formation is an indication of a change of the density of unoccupied states in the corresponding cyano orbitals. We will return to this point when discussing a complementary behavior found for the oxygen pre-edge resonances of the donor molecules. For the TTF-TCNQ complex, only small variations in nitrogen K-edge NEXAFS spectra in comparison with pure, neutral TCNQ have been observed.[14]

Oxygen K-Edge NEXAFS. The right panel of Figure 1 shows a series of spectra for the oxygen K-edge, with (e) and (g) corresponding to the identical samples as (a) and (c) in the left panel. Spectra (d) and (f) have been taken for pure HMP and TMP, respectively. Signals F−K were determined by the fit routine. As for nitrogen, the intensity differences in the pre-edge region (signals F and G) of the spectra of the pure donors and the complexes are evident.

The prominent resonance F at about 532 eV in spectra (e) and (g) (fwhm 900 meV) is separated by 3 eV from the next signal G. The energy position is in very good agreement with the position of the lowest-lying resonance measured by Amemiya et al. for the surface methoxy species on Cu (531.7 eV).[18] It derives from the highest occupied molecular orbital (HOMO) of the methoxy group. For an isolated methoxy group, this orbital has 2e-symmetry (2-fold degenerate) and is largely oxygen 2p-like (lone pair). According to a density functional theory (DFT) calculation,[5] the signature of 2e (see bottom left panel in Figure 2) shows up in a group of orbitals (HOMO-3 to HOMO-5), with the symmetry being reduced to a and b_3 (a and b) for TMP (HMP). Since signal F occurs at this energy, we assign it to the transitions F: O 1s → a, b_3 and O 1s → a, b (π *methoxy*) for TMP and HMP, respectively. In spectrum (d), corresponding to pure HMP, signal F is very weak, and in spectrum (f), for pure TMP, it is completely absent. This is not surprising because the final-state orbital of the NEXAFS resonant transition derives from the HOMO orbital of the functional group, which is completely occupied in the neutral species.

However, in the spectra of the complexes (e and g), signal F is significant; that is, the corresponding NEXAFS transition channel opens. Since the 2e-derived wave functions have their maximum amplitude at the oxygen atom, there is a large overlap of initial- and final-state wave functions in the matrix element (essentially O 1s → 2p). Thus, the oscillator strength of transition F is very high. For surface methoxy on Ni(111) and Cu(111), this transition is also significant, indicating a reduced occupation of the 2e-orbital due to the chemical bond to the transition metal.[18] The signal intensity of F is thus a measure for the unoccupied density of states in the 2e-derived orbitals.

The second signal G at about 535 eV (fwhm 1150 meV) is also higher in the spectra of the complexes. By analogy with the surface methoxy species,[18] we conclude that this signal derives from the 6a_1 orbital of the methoxy group with essentially σ^*(C−O) character. We denote the transitions as G: O 1s → a, b (σ^* methoxy), noting that in this case a and b derive from methoxy 6a_1 (being also observed for the methoxy species on Cu and Ni and for multilayer films of methanol).[18] Its intensity behavior is similar to that of signal F (see below). The remaining signals H, I, and K occur with similar intensities in all spectra. They correspond to transitions into orbitals of the aromatic ring system. The enhanced widths reflect the higher delocalization with increasing final state energy.

The strong intensity changes in signals F and G are an indicator of the unoccupied density of states in the frontier orbitals of the methoxy group. For pure donor material, signal F is practically absent, whereas it dominates the pre-edge spectrum for TMP-TCNQ (spectrum g).

Besides the strong intensity effect, the fit revealed systematic energetic shifts (see vertical lines, denoting peak maxima in Figure 1). Upon complex formation, all resonances associated with the donor molecules (right panel) shift to higher photon

dx.doi.org/10.1021/ja2100802 | J. Am. Chem. Soc. 2012, 134, 4694−4699

energies by up to 750 meV and all resonances associated with the acceptor (left panel) shift to lower photon energies by up to 120 meV.

We now quantify the eye-catching intensity variations and energy shifts of the pre-edge resonances. Figure 3 shows the

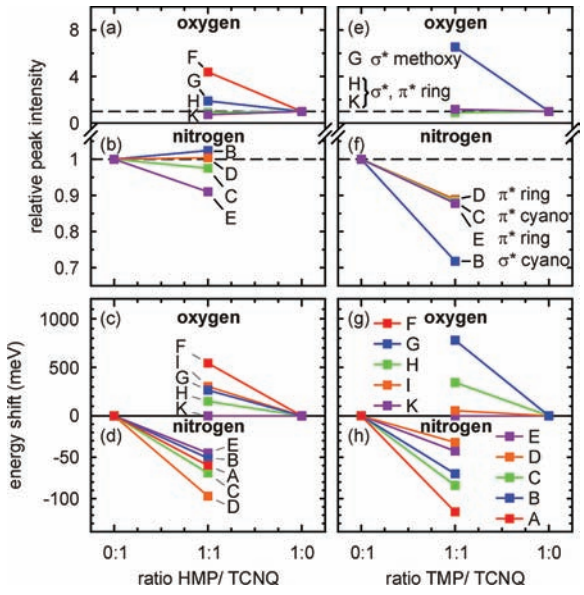

Figure 3. NEXAFS resonance intensities (peak areas as derived from the fits in Figure 1) in the oxygen (a, e) and nitrogen spectra (b, f) and corresponding energy shifts (c, g) and (d, h) as a function of the HMP/TCNQ and TMP/TCNQ ratio. Intensities are normalized to the areas of signals A and I for oxygen and nitrogen, respectively.

intensity variations of the oxygen (a, e) and nitrogen resonances (b, f) as a function of the HMP(TMP)/TCNQ ratio. The intensities have been determined as areas under the corresponding fit curves in the spectra normalized to the area of peak A for nitrogen and peak I for oxygen. The intensities of signals A and I vary just proportionally to the nitrogen or oxygen content of the samples. The intensity variations are most pronounced for signals F and G in the oxygen spectra, being associated with the frontier orbitals π and σ^* of the methoxy group.

Both signals show a substantial increase when going from pure donor (ratio 1:0) to the complex (1:1). For TMP-TCNQ the relative intensity of signal F would be ∞, since F is absent in pure TMP. Signals H and K stay practically constant; that is, the orbitals located in the aromatic ring system retain their unoccupied DOS upon formation of the complex. The nitrogen signals show a *decrease* of intensities, associated with the frontier orbitals π^* and σ^* of the cyano group.

The systematic intensity variations of specific resonances in donors and acceptor give direct evidence of the participation of the corresponding final-state orbitals in the charge-transfer process. The intensity increase of the O 1*s* → *methoxy* (π *and* σ^*) transitions in the complex reflects an unoccupied density of states in orbitals with contributions from the HOMO of the functional group of the donor. Amemiya et al.[18] determine a loss of charge from 4 electrons to 3.6 electrons in the 2*e*-orbital of the surface methoxy species on copper, associated with a pronounced 2*e*-derived pre-edge NEXAFS peak. Vice versa, the intensity loss of the N 1*s* → *cyano* (b_{1g}, b_{2u}, *and* b_{3g}, a_u) transitions indicates hybridization of these orbitals located at the functional C≡N group of the acceptor with occupied states from the π-system, resulting in a gain of charge in orbitals located at the cyano group.

Figure 2 illustrates the results in terms of a transition scheme including the orbitals involved in the charge transfer. The methoxy group promotes the donor character of HMP and TMP. In CT complexes a fractional amount of charge is transferred from donor to acceptor (horizontal arrow). This means that the probabilities to find an electron in the orbitals being involved in the charge transfer deviate from integer values. The present measurements show that the orbitals located at the functional groups are strongly involved in that process. The unoccupied DOS in donor orbitals derived from the frontier orbitals of the methoxy group (2*e* and $6a_1$) increases because partial charge is donated. For the acceptor the DOS of orbitals located at the cyano group (b_{3g} and a_u and b_{1g} and b_{2u}) decreases because partial charge is accepted. Although the π-orbitals of the ring systems mediate the charge transfer, their occupation numbers are less affected.

We can also adopt a different view on the opening of the transition channel to the 2*e*-derived state. Excitations into formally occupied orbitals have previously been observed by Grioni et al.[19] for various Cu^I compounds. Strong transition intensities observed at the Cu $L_{2,3}$ edges give evidence of transitions into hybridized states with partial d-character at the Cu atom in many compounds that formally should have the d^{10} atomic configuration. This is interpreted in terms of Cu 3*d*-4*s* hybridized states, sharing electrons in covalent bonds with ligands and thus allowing for transitions into "completely" occupied 3*d* states. We can apply a similar interpretation to our case: The methoxy 2*e*-derived orbital should be completely occupied. Due to hybridization with the π-system, however, the unoccupied molecular orbitals forming the π-system adopt a large projection integral with the O 2*p*-orbitals that formerly contributed to the methoxy 2*e*-orbital. Thus, these unoccupied orbitals become allowed as final states for the NEXAFS transitions. The absence of the 2*e*-derived signals in the pure donor samples gives evidence of full occupation and no hybridization with the π-system in the neutral species. The same behavior was found for multilayer methanol.[18]

In this picture, the strong increase of signals F and G indicates a strong increase of hybridization of the corresponding orbitals. The charge transfer between donor and acceptor shifts the peak energy mainly due to the varied screening effect on the nuclear charge; see the Supporting Information.

A calculation based on DFT was performed in order to analyze the band structure and DOS of the charge transfer salts and its constituents. The calculation was done for the crystal structures determined by X-ray diffraction. We use the full potential local orbital basis set[20] and the generalized gradient approximation functional in its Perdew, Burke, Ernzerhof form.[21] Figures 4 and 5 show the results for the complexes and the pure donors and acceptor.

The comparison of theory and experiment is straightforward in the case of TMP-TCNQ (Figure 4). For the case of HMP-TCNQ, calculations are performed for HMP-TCNQ·DMSO (Figure 5) because structure data are only available for the DMSO intercalated cocrystals. Since the coarse DOS features of TMP-TCNQ and HMP-TCNQ·DMSO look similar and DMSO orbitals do not hybridize with HMP or TCNQ orbitals, theoretical results for HMP-TCNQ·DMSO can be compared with experimental results for HMP-TCNQ.

We observe that the charge transfer salts have small gaps of 0.37 eV (TMP-TCNQ) and 0.39 eV (HMP-TCNQ·DMSO)

dx.doi.org/10.1021/ja2100802 | *J. Am. Chem. Soc.* 2012, 134, 4694–4699

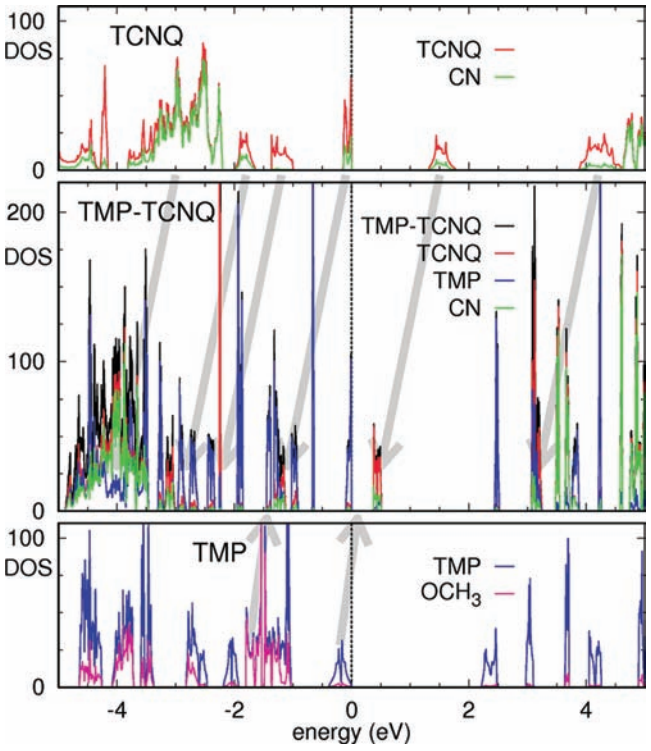

Figure 4. Calculated density of states of TMP-TCNQ (middle panel) compared to that of TCNQ (top) and TMP (bottom). The Fermi level is indicated by a dashed line. In our calculations, the Fermi level is chosen to be at the top of the valence band.

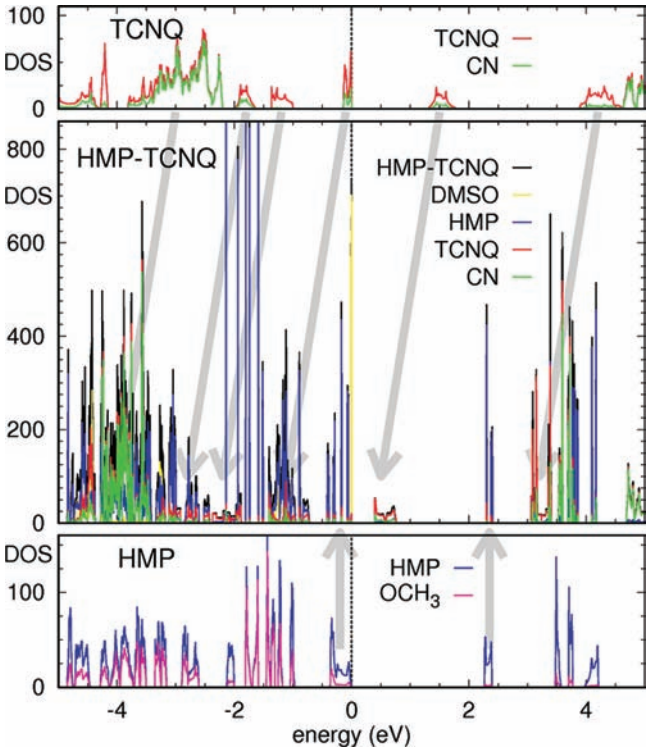

Figure 5. Same as Figure 4 but for HMP-TCNQ·DMSO. Note that, for HMP-TCNQ·DMSO, number of formula units per unit cell $Z = 4$ while, for pure TCNQ and HMP, $Z = 2$.

while the crystals of the pure components have large gaps of 2.2 eV (TMP), 2.3 eV (HMP), and 1.3 eV (TCNQ). The contributions of TMP (HMP) are shown in blue (middle and bottom panels), those of TCNQ in red (top and middle panels), those of the CN groups in green, and those of the methoxy groups in purple. The effect of the charge transfer is seen in the lowest unoccupied states of TCNQ; they are shifted as suggested by the gray arrows and partly occupied while hybridizing with the highest occupied states of TMP (HMP). Consequently, the highest occupied states of the TMP-TCNQ complex have some admixture of TCNQ/cyano group character, and the lowest unoccupied states of the complex have contributions from the TMP(HMP)/methoxy group, as detected experimentally. This hybridization acts on the NEXAFS transitions and gives rise to the observed intensity changes. The direction and order of magnitude of the calculated energy shifts are in agreement with the measured shifts (Figure 3c,d,g,h). However, the ground state calculations cannot account for final state screening effects in the NEXAFS transition; see also the Supporting Information.

The calculation allows estimating the degree of charge transfer in two different ways: From the charge density we find an overall charge transfer of 0.13 (0.17) electrons per formula unit from TMP (HMP) to TCNQ. These values agree roughly with the 0.16 (0.33) electrons TCNQ contribution to the highest occupied, TMP (HMP)-derived bands of the complex and with the 0.21 (0.31) electrons TMP (HMP) contribution to the lowest unoccupied, TCNQ derived bands. We note that these values are somewhat underestimating the true degree of charge transfer due to the fact that the generalized gradient approximation has a tendency to distribute the charges as evenly as possible.

CONCLUSIONS

Near-edge X-ray absorption fine structure (NEXAFS) spectroscopy was established as a tool to study the orbital-specific charge transfer in novel donor−acceptor complexes. The functionalized pyrene-derivatives *4,5,9,10-tetramethoxypyrene* (TMP) and *2,4,5,7,9,10-hexamethoxypyrene* (HMP) were employed as donors in complexes with the classical acceptor *7,7,8,8-tetracyano-p-quinodimethane* (TCNQ). TMP-TCNQ and HMP-TCNQ crystals were grown by vapor diffusion.

Oxygen and nitrogen K-edge NEXAFS spectra were exploited to probe the functional groups of the donor and acceptor moieties, respectively. Oxygen is only contained in the methoxy groups of the donor and nitrogen in the cyano groups of the acceptor. The orbital selectivity of the NEXAFS resonances allowed elucidating the participation of specific orbitals in the charge-transfer process. Strong intensity changes in the oxygen K-edge spectra occur upon formation of the complex. They reveal an increased hybridization of the frontier orbitals of the functional group of the donor (having symmetry $2e$ and $6a_1$ in an isolated methoxy group) with π^*-orbitals of the ring system in the complex. The nitrogen K-edge spectra show a similar effect of opposite sign in the acceptor moiety, i.e. a marked intensity drop of the transitions into the states b_{3g} and a_u (π^*) and b_{1g} and b_{2u} (σ^*), located at the cyano group. The π-orbitals of the aromatic ring system mediate the charge transfer, but the transition strengths into these orbitals change much less than into those located at the functional groups. The resonance positions show significant shifts as well: upon complex formation the positions of resonances starting from oxygen 1*s* (donor) and nitrogen 1*s* (acceptor) shift to higher and lower photon energies, respectively. These shifts are a consequence of the charge transfer between the moieties, as is evident from the calculation (Figures 4 and 5).

dx.doi.org/10.1021/ja2100802 | *J. Am. Chem. Soc.* 2012, 134, 4694−4699

Providing quantitative access to the unoccupied density of states of specific orbitals and the charge transfer between donor and acceptor, the NEXAFS can shine new light into the nature of the charge-transfer mechanism in organic salts. A strong intensity increase of the oxygen pre-edge features for both complexes is interpreted as a fingerprint of additional hole states in the functional group of the donor in the CT complex. In particular, the most prominent pre-edge feature is even absent in the spectra of pure donor material. This gives evidence of strong participation of the HOMO of the methoxy group in the charge transfer. Vice versa, NEXAFS resonances of the acceptor TCNQ appear significantly weaker in the complex, indicating partial filling of these states in the acceptor. The effect of the methoxy groups ("pushing charge into the π-system") thus clearly shows up in terms of opening of the $1s \rightarrow 2e$ transition channel, associated with the occurrence of a new NEXAFS pre-edge resonance, 3 eV below the next signal. This happens only in the CT complex, where the donors actually loose charge, but not in the neutral donors. Thus, NEXAFS spectra give an unprecedented access to details of the CT mechanism. Our experimental observation that several orbitals are involved in the charge transfer process is qualitatively explained by means of a theoretical calculation based on density functional theory.

Although demonstrated for the specific example of pyrene-derived donors with the classical acceptor TCNQ, the method is very versatile and can serve as a routine spectroscopic tool for novel CT complexes on the basis of functionalized polycyclic aromatic hydrocarbons. NEXAFS thus complements the classical techniques of probing charge-transfer in complexes, such as infrared spectroscopy (giving access to a red-shift of the C≡N stretching frequency upon complex formation)[5] or optical measurements determining the band gap in the complex.

■ ASSOCIATED CONTENT

Ⓢ Supporting Information

Supporting figures on CT complexes in solution, on the crystal structure, and on the energy shifts of NEXAFS resonances. This material is available free of charge via the Internet at http://pubs.acs.org.

■ AUTHOR INFORMATION

Corresponding Author

medyanyk@uni-mainz.de

Notes

The authors declare no competing financial interest.

■ ACKNOWLEDGMENTS

The project is funded through Transregio SFB TR 49 (Frankfurt, Mainz, Kaiserslautern), Helmholtz Association (HA216/EMMI), Graduate School of Excellence MAINZ, and Centre for Complex Materials (COMATT), Mainz. We thank C. Felser, S. Naghavi (Inst. for Inorganic and Analytical Chemistry, Univ. Mainz) as well as M. Huth, V. Solovyeva, and M. Rudloff (Univ. of Frankfurt/Main) for fruitful cooperation. We acknowledge the Angstromquelle Karlsruhe (ANKA) for the provision of beam time.

■ REFERENCES

(1) Wu, J.; Pisula, W.; Müllen, K. *Chem. Rev.* **2007**, *107*, 718.
(2) Rieger, R.; Kastler, M.; Enkelmann, V.; Müllen, K. *Chem.—Eur. J.* **2008**, *14*, 6322.
(3) Medjanik, K.; Kutnyakhov, D.; Nepijko, S. A.; Schönhense, G.; Naghavi, S.; Alijani, V.; Felser, C.; Koch, N.; Rieger, R.; Baumgarten, M.; Müllen, K. *Phys. Chem. Chem. Phys.* **2010**, *12*, 7184.
(4) Clar, E.; Schmidt, W. *Tetrahedron* **1976**, *32*, 2563.
(5) Medjanik, K.; Perkert, S.; Naghavi, S.; Rudloff, M.; Solovyeva, V.; Chercka, D.; Huth, M.; Nepijko, S. A.; Methfessel, T.; Felser, C.; Baumgarten, M.; Müllen, K.; Elmers, H. J.; Schönhense, G. *Phys. Rev. B* **2010**, *82*, 245419.
(6) Rochet, F.; Bournel, F.; Gallet, J.-J.; Dufour, G.; Lozzi, L.; Sirotti, F. *J. Phys. Chem. B* **2002**, *106*, 4973.
(7) Chen, W.; Chen, Q. D.; Li, H. Q.; Huang, H.; Zhan, W. Y.; Chen, S.; Yu, G. X.; Thye, S. W. A. *J. Phys. Chem. C* **2009**, *113*, 12839.
(8) Miyamoto, T.; Kitajima, Y.; Sugawara, H.; Naito, T.; Inabe, T.; Asakura, K. *J. Phys. Chem. C* **2009**, *113*, 20480.
(9) Bässler, M.; Fink, R.; Buchberger, C.; Väterlein, P.; Jung, M.; Umbach, E. *Langmuir* **2000**, *16*, 6681.
(10) Hünig, S.; Herberth, E. *Chem. Rev.* **2004**, *104*, 5563.
(11) Peisert, H.; Biswas, I.; Zhang, L.; Schuster, B.-E.; Casu, M. B.; Haug, A.; Batchelor, D.; Knupfer, M.; Chassé, T. *J. Chem. Phys.* **2009**, *130*, 194705.
(12) Stöhr, J. *NEXAFS spectroscopy*; Springer Series in Surface Science *25*; Springer: Heidelberg, 1992.
(13) Tseng, T.-C.; Urban, C.; Wang, Y.; Otero, R.; Tait, S. L. *Nature Chem.* **2010**, *2*, 374.
(14) Fraxedas, J.; Lee, Y. J.; Jimenez, I.; Gago, R.; Nieminen, R. M.; Ordejon, P.; Canadell, E. *Phys. Rev. B* **2003**, *68*, 195115.
(15) Sing, M.; Schwingenschlögl, U.; Claessen, R.; Blaha, P.; Carmelo, J. M. P.; Martelo, L. M.; Sacramento, P. D.; Dressel, M.; Jacobsen, C. S. *Phys. Rev. B* **2007**, *76*, 245119.
(16) Claessen, R.; Sing, M.; Schwingenschlögl, U.; Blaha, P.; Dressel, M.; Jacobsen, C. S. *Phys. Rev. Lett.* **2002**, *88*, 096402.
(17) Sing, M.; Schwingenschlögl, U.; Claessen, R.; Blaha, P.; Carmelo, J. M. P.; Martelo, L. M.; Sacramento, P. D.; Dressel, M.; Jacobsen, C. S. *Phys. Rev. B* **2003**, *68*, 125111.
(18) Amemiya, K.; Kitajima, Y.; Yonamoto, Y.; Terada, S.; Tsukabayashi, H.; Yokoyama, T.; Ohta, T. *Phys. Rev. B* **1999**, *59*, 2307.
(19) Grioni, M.; Goedkoop, J. B.; Schoorl, R.; de Groot, F. M. F.; Fuggle, J. C.; Schäfers, F.; Koch, E. E.; Rossi, G.; Esteva, J.-M.; Karnatak, R. C. *Phys. Rev. B* **1989**, *39*, 1541.
(20) Koepernik, K.; Eschrig, H. *Phys. Rev. B* **1999**, *59*, 1743.
(21) Perdew, J. P.; Burke, K.; Ernzerhof, M. *Phys. Rev. Lett.* **1996**, *77*, 3865.